Suplemento de la Revista Mexicana de Física **6** 011301 (2025) 1–9

Applications of information theory to compact objects: configurational entropy as a stability criterion

P.S. Koliogiannis[a,b], M. Vikiaris[b], G. Tsalis[b], C. Panos[b], V. Petousis[c], M. Veselský[c], and Ch.C. Moustakidis[b]

[a]*Department of Physics, Faculty of Science, University of Zagreb, Bijenička cesta 32, 10000 Zagreb, Croatia.*

[b]*Department of Theoretical Physics, Aristotle University of Thessaloniki, 54124 Thessaloniki, Greece,*

[c]*Institute of Experimental and Applied Physics, Czech Technical University, Prague, 110 00, Czechia*

Received 18 February 2025; accepted 7 March 2025

M. Gleiser and N. Jiang [Phys. Rev. D **92**, 044046, 2015] established that, within the simple Fermi gas model and self–gravitating complex scalar field configurations, the stability regions of neutron stars-determined using conventional perturbation techniques–align with the critical points of the configurational entropy, with deviations of only a few percent. Extending their work, we employ a range of realistic equations of state, suitable to describe neutron stars, quark stars, and hybrid stars (twin stars), to explore the potential correlation. Our findings indicate that, at least quantitatively, the proposed stability prediction lacks universal validity for neutron and quark stars. Furthermore, to enrich our analysis, we compute the configurational entropy for fermionic and bosonic systems (interacting Fermi and boson gases), revealing a strong correlation between the stability points predicted by configurational entropy and those obtained through traditional methods, with a slight dependence on interaction strength. In conclusion, configurational entropy can be a valuable tool for studying compact object stability, though its predictive accuracy depends on the specific equation of state.

Keywords: Configurational entropy; stability condition; compact objects; equation of state.

DOI: https://doi.org/10.31349/SuplRevMexFis.6.011301

1. Introduction

In recent years, there has been significant interest in studying astrophysical objects using the concept of information entropy and related measures. Sañudo and Pacheco [1] explored the relationship between complexity and the structure of white dwarfs, while this approach was later extended to neutron star structures [2], revealing that neutron stars, within the current theoretical framework, are ordered systems. Similar studies took place in the following years in a series of papers [3–7] and Herrera *et al.* [8–11] refined the definition of complexity factors in self-gravitating systems, offering an alternative approach to the problem. Further applications of information measures can be found in Refs. [12–24]. A specific application of information measures is configurational entropy (CE), introduced by Gleiser and Stamatopoulos [25] to explore the link between dynamical and informational aspects of physical models with localized energy configurations. In the following years, CE has been applied in various related studies [26-36], where in one of them, Gleiser and Jiang [27] found that minimizing CE provides an alternative way to predict stability through the maximum mass configuration.

It is worth mentioning that the study of the longstanding problem of the stability of relativistic stars [36–42] is mainly carried out by the following three methods: (a) The approach for identifying the point corresponding to the minimum of the binding energy, defined as $E_B = (M - m_b N)c^2$ (where m_b is the mass of a single nucleon, M stands for the gravitational mass, and N is the total number of nucleons) [36–42]. (b) The variational method developed by Chandrasekhar [43,44], which assesses stability by examining small radial perturbations of the equilibrium state via the Sturm-Liouville eigenvalue equation. This yields a discrete series of eigenfrequencies ω_n [36] satisfying $\omega_n^2 < \omega_{n+1}^2$ for $n = 0, 1, 2, \ldots$, where ω_n being real numbers. If any ω_n^2 is negative, the perturbation grows exponentially, leading to stellar collapse. Stability is ensured only when all eigenfrequencies are positive. (c) The approach relying on the relationship between gravitational mass M and radius R with respect to the central energy density $\mathcal{E}_c$ (referred to as the traditional method, TM). According to this criterion, stability is ensured when the mass increases with rising central energy density, *i.e.*, $dM/d\mathcal{E}_c > 0$. A mass extreme signifies a transition in the stability of the compact star configuration [36–42]. It is crucial to highlight that these three methods converge when determining the stability point. Therefore, identifying this point using any of them guarantees the accuracy of the result.

Until now, no comprehensive study has systematically applied CE to the investigation of compact astrophysical objects. This work aims to build upon the limited existing research by exploring all potential natural objects through an alternative approach to assessing their stability. In particular, in the present work we make an effort to answer key questions, including whether CE minimization uniquely corresponds to the stability point across different EoSs, whether this relationship is universal or EoS-dependent, and whether stability can be linked to CE minimization in specific cases. Undoubtedly, discovering new approaches beyond classical methods for determining the stability of compact objects

is of great significance. To be more specific, we review and analyze the methodology and the results of our recent work [45, 46], where the third method to investigate the relationship between the stability of relativistic stars and CE is employed. Extending the findings of Ref. [27], we analyze the connection between neutron star properties and CE, with a particular focus on stability conditions. Using two analytical solutions of the Tolman-Oppenheimer-Volkoff (TOV) equations and a diverse set of realistic equations of state (EoSs), we explore various compact objects, including neutron stars, quark stars, and twin stars. Additionally, we present the calculation of the CE for fermionic and bosonic systems, modeled as interacting Fermi and boson gases in self-gravitating configurations [45, 46]. Our conclusions can be summarized as follows: while the proposed stability prediction lacks universal validity for neutron and quark stars, in the case of fermionic and bosonic systems a strong correlation exists between the stability points predicted by CE and those obtained through TM. As a main conclusion, CE serves as a valuable tool for analyzing the stability of compact objects, though its predictive accuracy is influenced by the chosen EoS.

The paper is organized as follows: in Sec. 2, we present the basic formalism of hydrodynamic equilibrium, followed by a review of the definition of configurational entropy in Sec. 3. The role of the analytical solutions and the parametrization of the EoSs are discussed in Sec. 4. The results of the present study are presented and analyzed in Sec. 5. Finally, Sec. 6 contains the concluding remarks.

2. Hydrodynamic equilibrium

To establish the corresponding configuration for each compact object – a crucial step in computing the CE – we utilize Einstein's field equations for a spherically symmetric fluid. In this context, the mechanical equilibrium of stellar matter is governed by the well-known TOV equations [36–39]

$$\frac{dP(r)}{dr} = -\frac{G\mathcal{E}(r)M(r)}{c^2r^2}\left(1+\frac{P(r)}{\mathcal{E}(r)}\right) \times \left(1+\frac{4\pi P(r)r^3}{M(r)c^2}\right)\left(1-\frac{2GM(r)}{c^2r}\right)^{-1}, \quad (1)$$

$$\frac{dM(r)}{dr} = \frac{4\pi r^2}{c^2}\mathcal{E}(r), \quad (2)$$

where $P(r)$ and $\mathcal{E}(r)$ are the pressure and energy density, respectively. The TOV equations are solved numerically by incorporating an EoS that describes the relationship between pressure and energy density, yielding the properties of neutron stars.

3. Configurational entropy

The key quantity to calculate the CE in momentum space is the Fourier transform $F(\mathbf{k})$ of the density $\rho(r) = \mathcal{E}(r)/c^2$, originating from the solution of the TOV equations, that is

$$F(\mathbf{k}) = \int\int\int \rho(r)e^{-i\mathbf{k}\cdot\mathbf{r}}d^3\mathbf{r}. \quad (3)$$

It is notable that the function $F(\mathbf{k})$ in the case of zero momentum, coincides with the gravitational mass of the compact object, that is $F(0) \equiv M$, since by definition (see Eq. (2))

$$M = 4\pi\int_0^R \rho(r)r^2dr. \quad (4)$$

Moreover, we define the modal fraction $f(\mathbf{k})$ [27]

$$f(\mathbf{k}) = \frac{|F(\mathbf{k})|^2}{\int |F(\mathbf{k})|^2 d^3\mathbf{k}}, \quad (5)$$

and also the function $\tilde{f}(\mathbf{k}) = f(\mathbf{k})/f(\mathbf{k})_{\max}$, where $f(\mathbf{k})_{\max}$ is the maximum fraction, which is given in many cases by the zero mode $k = 0$, or by the system's longest physics mode, $|k_{\min}| = \pi/R$. The above normalization guarantees that $\tilde{f}(\mathbf{k}) \leq 1$ for all values of $\mathbf{k}$. Finally, the CE, S_C, as a functional of $\tilde{f}(\mathbf{k})$, is given by

$$S_C[\tilde{f}] = -\int \tilde{f}(\mathbf{k})\ln[\tilde{f}(\mathbf{k})]d^3\mathbf{k}. \quad (6)$$

Summarizing, for each EoS, an infinite number of configurations can appear, leading to the construction of $M-\rho_c$ and S_C-ρ_c dependence. The latter facilitates the investigation of any possible correlation between the minimum of S_C and the stability point of compact objects under examination.

4. Equations of state

4.1. EoSs and analytical solutions

In general, to obtain realistic solutions, one must follow the procedure outlined in Sec. 2. However, an alternative approach uses the analytical solutions to the TOV equations, which are often of limited physical relevance. While many such solutions have been found, only a few are significant. This work focuses on two important solutions: the Schwarzschild (constant-density) and Tolman-VII solutions

- **Schwarzschild solution**: In the case of the Schwarzschild interior solution, the density is constant throughout the star [40, 41]. The energy density and the pressure read as

$$\mathcal{E} = \mathcal{E}_c = \frac{3M}{4\pi R^3}, \quad (7)$$

$$\frac{P(x)}{\mathcal{E}_c} = \frac{\sqrt{1-2\beta}-\sqrt{1-2\beta x^2}}{\sqrt{1-2\beta x^2}-3\sqrt{1-2\beta}}, \quad (8)$$

where $x = r/R$, $\beta = GM/Rc^2$ is the compactness of the star, and $\mathcal{E}_c = \rho_c c^2$ is the central energy density.

- **Tolman-VII solution**: The Tolman-VII solution has been extensively employed in neutron star studies [47–51]. The energy density and the pressure read as [51]

$$\frac{\mathcal{E}(x)}{\mathcal{E}_c} = (1-x^2), \quad \mathcal{E}_c = \frac{15Mc^2}{8\pi R^3}, \tag{9}$$

$$\frac{P(x)}{\mathcal{E}_c} = \frac{2}{15}\sqrt{\frac{3e^{-\lambda}}{\beta}}\tan\phi - \frac{1}{3} + \frac{x^2}{5}. \tag{10}$$

Analytical solutions are valuable as they provide explicit expressions for key quantities and serve as a means to verify numerical calculations. These solutions apply to any compact object, regardless of mass or radius, making them useful for studying both massive and supramassive objects governed by the TOV equations. Analytical solutions provide valuable insights into the qualitative and quantitative behavior of CE as a function of central density ρ_c.

4.2. Hadronic EoSs

For the description of neutron stars, we use a set of hadronic EoSs, which have been extensively employed in the literature for applications in neutron star properties (see Ref. [52] and references therein). These EoSs have been collected in order to satisfy the prediction of the maximum observed neutron star mass, that is, $M \geq 2M_\odot$. In this case, for a specific EoS and for each M-R configuration, we implement the corresponding density distribution $\rho(r)$. Afterwards, the calculation of $F(k)$, $f(k)$, and $\tilde{f}(k)$ is performed according to the presented recipe. It has to be mentioned that it is well established that the stability point corresponds to the configuration of the maximum mass [38].

4.3. Quark EoSs

For the description of quark stars, we utilize a set of EoSs for interacting quark matter, as predicted and applied in Ref. [53]. In this scenario, the pressure is connected to the energy density through the simplified expression

$$\frac{P}{4B_{\rm eff}} = \frac{1}{3}\left(\frac{\mathcal{E}}{4B_{\rm eff}} - 1\right) + \frac{4}{9\pi^2}\bar{\lambda} \times \left(-1 + \sqrt{1 + \frac{3\pi^2}{\bar{\lambda}}\left[\frac{\mathcal{E}}{4B_{\rm eff}} - \frac{1}{4}\right]}\right). \tag{11}$$

Specifically, in the present work we employed the value of $B_{\rm eff} = 150$ MeV fm^{-3}, while for the dimensionless parameter $\bar{\lambda}$, we applied the values of $(1, 2, 5, 16)$ [53].

4.4. Hybrid EoSs

For the description of hybrid stars, we adopt a more sophisticated EoS designed to replicate the characteristics of a third family of compact objects, known as twin stars [42,54]. Specifically, we utilize the Maxwell construction, which is well-suited for describing phase transitions within a compact object and is formulated as follows [54].

$$\mathcal{E}(P) = \begin{cases} \mathcal{E}(P), & P \leq P_{\rm tr}, \\ \mathcal{E}(P_{\rm tr}) + \Delta\mathcal{E} + c_s^{-2}(P - P_{\rm tr}), & P \geq P_{\rm tr}, \end{cases} \tag{12}$$

where $c_{\rm s} = \sqrt{\partial P/\partial\mathcal{E}}$ is the speed of sound (in units of the speed of light), and $\Delta\mathcal{E}$ is the magnitude of the energy density jump at the transition point. The subscript "tr" denotes the corresponding quantity at this point. In the region $P \leq P_{\rm tr}$, we utilized the GRDF-DD2 EoS [55, 56] while in the region $P \geq P_{\rm tr}$, the value of the speed of sound is fixed at $c_{\rm s} = 1$.

4.5. Interacting Fermi gas (FG)

For compact objects composed solely of interacting Fermi gas (FG), we considered the simplest extension of the free fermion gas by adding an extra term that introduces repulsive interactions between the fermions. As a result, the energy density and pressure of the fermions are described as follows (for a detailed analysis, see Ref. [57])

$$\mathcal{E}(n_\chi) = \frac{(m_\chi c^2)^4}{(\hbar c)^3 8\pi^2}\Big[x\sqrt{1+x^2}(1+2x^2) - \ln(x+\sqrt{1+x^2})\Big] + \frac{y^2}{2}(\hbar c)^3 n_\chi^2, \tag{13}$$

$$P(n_\chi) = \frac{(m_\chi c^2)^4}{(\hbar c)^3 8\pi^2}\Big[x\sqrt{1+x^2}(2x^2/3-1) + \ln(x+\sqrt{1+x^2})\Big] + \frac{y^2}{2}(\hbar c)^3 n_\chi^2, \tag{14}$$

where m_χ is the particle mass, considered equal to $m_\chi = 939.565$ MeV/c^2 for reasons of simplicity (this holds throughout the study), n_χ is the number density and

$$x = \frac{(\hbar c)(3\pi^2 n_\chi)^{1/3}}{m_\chi c^2}.$$

The last parameter, y (in units of MeV^{-1}), is the one that introduces the repulsive interaction. In this study we have considered the values $y = [0, 0.001, 0.005, 0.01, 0.05, 0.1, 0.3, 0.5]$ (MeV^{-1}) where increasing y increases the strength of the interaction and vice-versa.

4.6. Interacting boson gas (BG)

Since the construction of the EoS for the boson gas is not uniquely determined, we present three cases based on different assumptions. It is important to note that, because the scalar field only vanishes at spatial infinity, boson stars do not have a defined radius where the energy density and pressure drop to zero. Therefore, we do not apply a momentum cut-off scheme, $0 \leq |\mathbf{k}| \leq \infty$.

1. **BG-C1**:The EoS of boson stars with repulsive interactions was first derived in Refs. [58–60], and has since been widely used in relevant calculations. Specifically, the energy density is given as

$$\mathcal{E}(P) = \frac{4}{3w}\left[\left(\sqrt{\frac{9w}{4}}P + 1\right)^2 - 1\right], \qquad (15)$$

where the interaction parameter w is equal to $w = 4\lambda(\hbar c)^3/(m_\chi c^2)^4$ (in units of MeV^{-1} fm^3). In this study, we have considered the values $w = [0.001, 0.005, 0.01, 0.05, 0.1, 0.3, 0.5]$ $(\mathrm{MeV}^{-1}$ $\mathrm{fm}^3)$ where increasing w increases the strength of the interaction and viceversa.

2. **BG-C2**: The interior of a boson star can also be described using the EoS provided in Ref. [61], which was recently applied in Ref. [62], where the energy density is expressed as

$$\mathcal{E}(P) = P + \sqrt{\frac{2P}{z}}, \qquad (16)$$

with the interaction parameter z being equal to $z = u^2(\hbar c)^3/(m_\chi c^2)^2$ (in units of MeV^{-1} fm^3). In this study, we have considered the values $z = [0.001, 0.005, 0.01, 0.05, 0.1, 0.3, 0.5]$ $(\mathrm{MeV}^{-1}$ $\mathrm{fm}^3)$.

3. **BG-C3**: In Ref. [63], the authors investigated self-interacting boson stars with various scalar potentials and found that their properties differ significantly from previous calculations. To improve the link between the stability criterion and the CE, we used two EoS cases introduced in Ref. [63]: (a) one with a mass term (MT) and (b) one with a vacuum term (VT) without a mass term. The scaling EoSs are expressed as

$$\mathcal{E}(P) = \begin{cases} P^{2/n} + (n+2)P/(n-2), & \text{MT} \\ 1 + (n+2)P/(n-2), & \text{VT} \end{cases} \qquad (17)$$

where the index n is restricted to $n > 2$. In this study, we have considered the values $n = [4, 5]$ for MT [hereafter case (a)] and $n = [3, 4, 5]$ for VT [hereafter case (b)]. Another reason for using the mentioned cases is that they produce different mass-radius diagrams (depending on the index values), thereby covering a broad range of scenarios that could correspond to boson stars.

5. Results and discussion

5.1. Neutron stars

We first examine the relationship between gravitational mass, radius, and CE for hadronic EoSs, as shown in Fig. 1. The results indicate that the stability point, determined by the TM, does not coincide with the CE minimum. A possible explanation is that the existence of the crust in the outer envelope of neutron stars, with a specific structure, may have a dramatic effect on locating the stability point by the CE minimization method. In some cases, no clear CE minimization is observed, even at high central densities. Generally, CE decreases with central density, and its minimum occurs in the instability region of neutron stars. However, in one special case–the free Fermi gas–the CE minimum and stability point nearly coincide.

5.2. Quark stars-Hybrid stars

Quark stars differ from neutron stars in structure, as their surface density remains non-zero even when pressure vanishes. This affects the mass-radius relationship. For the four EoSs studied, the CE minimum and TM stability points do not align, as shown in Fig. 2. In this case, where there is no crust, the failure of the method does not currently have a solid explanation. In the case of twin (hybrid) stars, shown in

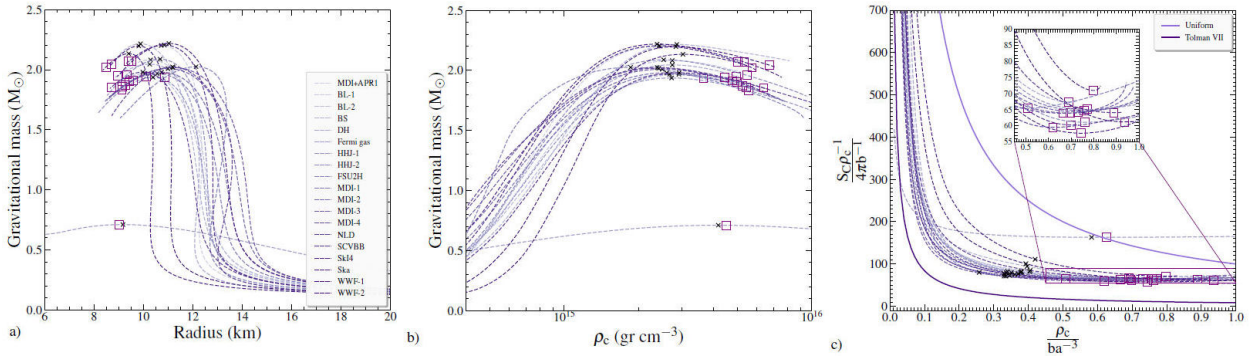

FIGURE 1. a) Gravitational mass as a function of the radius for a set of hadronic EoSs. b) The corresponding dependence of the gravitational mass as a function of the central density. c) The corresponding configurational entropy as a function of the central density and two analytical solutions of TOV equations (a and b are constants to ensure dimensionless units; for more details see Refs. [45, 46]). The inset figure indicates the location of the minimization of the CE. The black crosses indicate the stability points due to the TM while the open squares correspond to the minimum of the CE. The hadronic EoSs are presented with the dashed lines, and the analytical solutions with the solid ones.

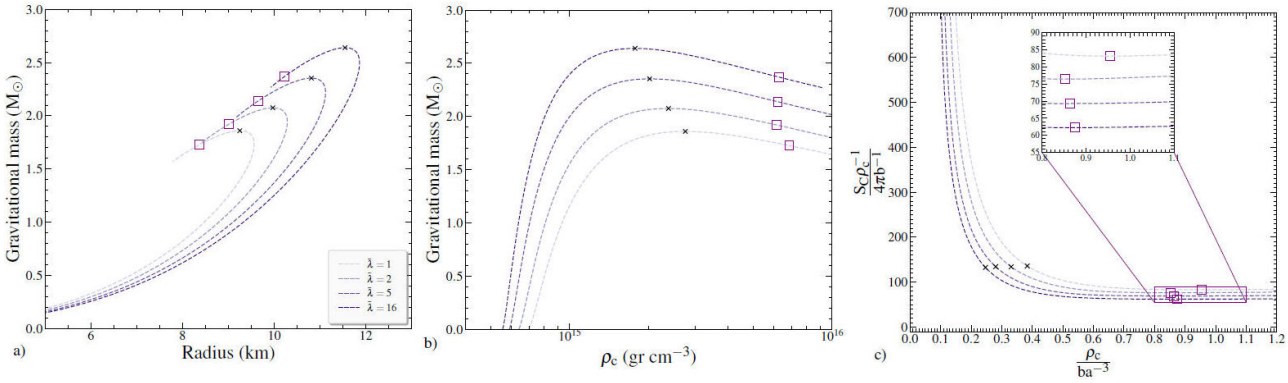

FIGURE 2. Same as the caption of Fig. 1, but for a set of quark star EoSs.

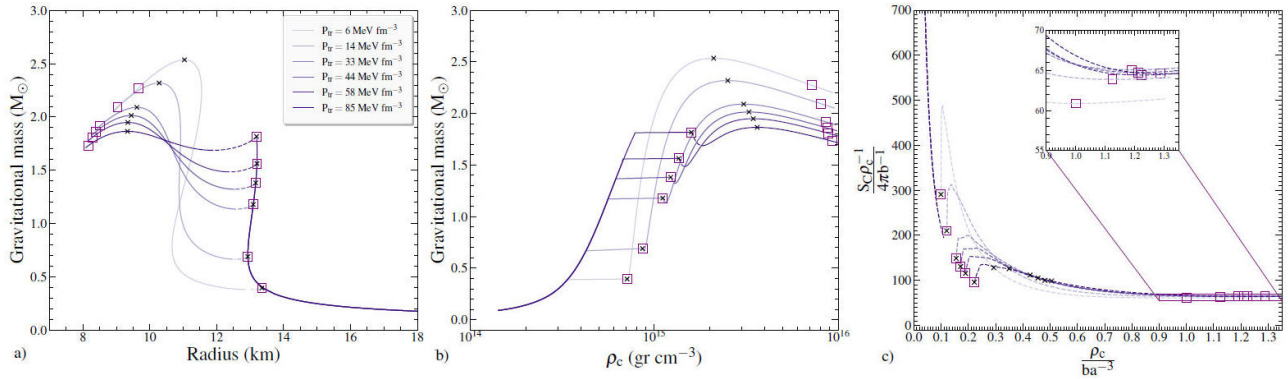

FIGURE 3. Same as the caption of Fig. 1, but for a set of twin-star EoSs.

Fig. 3, two stability points exist for the six EoSs. The first CE minimum closely matches the first stability point but is likely an artifact of an EoS discontinuity. The second CE minimum, however, remains significantly distant from the second stability point, occurring at much higher central densities.

5.3. Fermion and boson stars

Moving on to fermionic and bosonic EoSs, we present in Fig. 4 four cases: FG, BG-C1, BG-C2, and BG-C3. In the case of the FG, the first panel of Fig. 4 displays that the points due to TM and CE are located in proximity, validating the CE method for the location of the stability point. Error analysis of key quantities (gravitational mass, radius, central density, and compactness) shows that while the error in gravitational mass is below 5%, the central density error can reach nearly 99%, depending on the interaction value. This issue arises from a plateau after the rapid decrease of CE, which keeps CE narrow while central density spans a wide range. No clear pattern links interaction strength to error. While CE can accurately estimate the maximum gravitational mass, it encounters difficulties in determining the central density. In some cases, CE fails to identify the total minimum, finding a local minimum near the maximum mass configuration instead, a result consistent across all cases studied. In any case, we hypothesize that the accuracy of the CE minimization method in predicting the stability point is partly attributed to the use of a single EoS for the entire star. This contrasts with neutron stars, where separate EoSs are used for the core and the crust.

In the BG case, a similar behavior to the FG is observed.

The difference between TM and CE points is minimal, but error analysis shows that, like in the FG case, the error in gravitational mass is under 5%, while the error in central density can reach up to 100%. While CE can estimate the maximum mass, it cannot accurately determine the associated central density. This behavior in both FG and BG cases reinforces the idea that the stability point's location is an intrinsic property of the EoS.

Finally, it is worth mentioning here that the primary distinction between fermionic and bosonic systems lies in the choice of the momentum cutoff scheme. Specifically, we considered two cutoff schemes: (a) $k_{\min} = \pi/R$, which is based on the radius of the boson star originated from the condition that the pressure vanishes at the star's surface, $P(R) = 0$, and (b) $k_{\min} = \pi/R_{\rm eff}$, which is the effective radius where most of the star's mass is concentrated and defined as [27] $R_{\rm eff} \equiv \int_0^\infty \rho(r) r^3 dr / \int_0^\infty \rho(r) r^2 dr$. Figure 5 illustrates the impact of the cut-off scheme for the BG-C1 (0.001) EoS as a representative case, showing a substantial enhancement in accuracy. In particular, case (a) exhibits a notable improvement compared to the no cutoff case, consistent with the results of other cases [45, 46]. Furthermore,

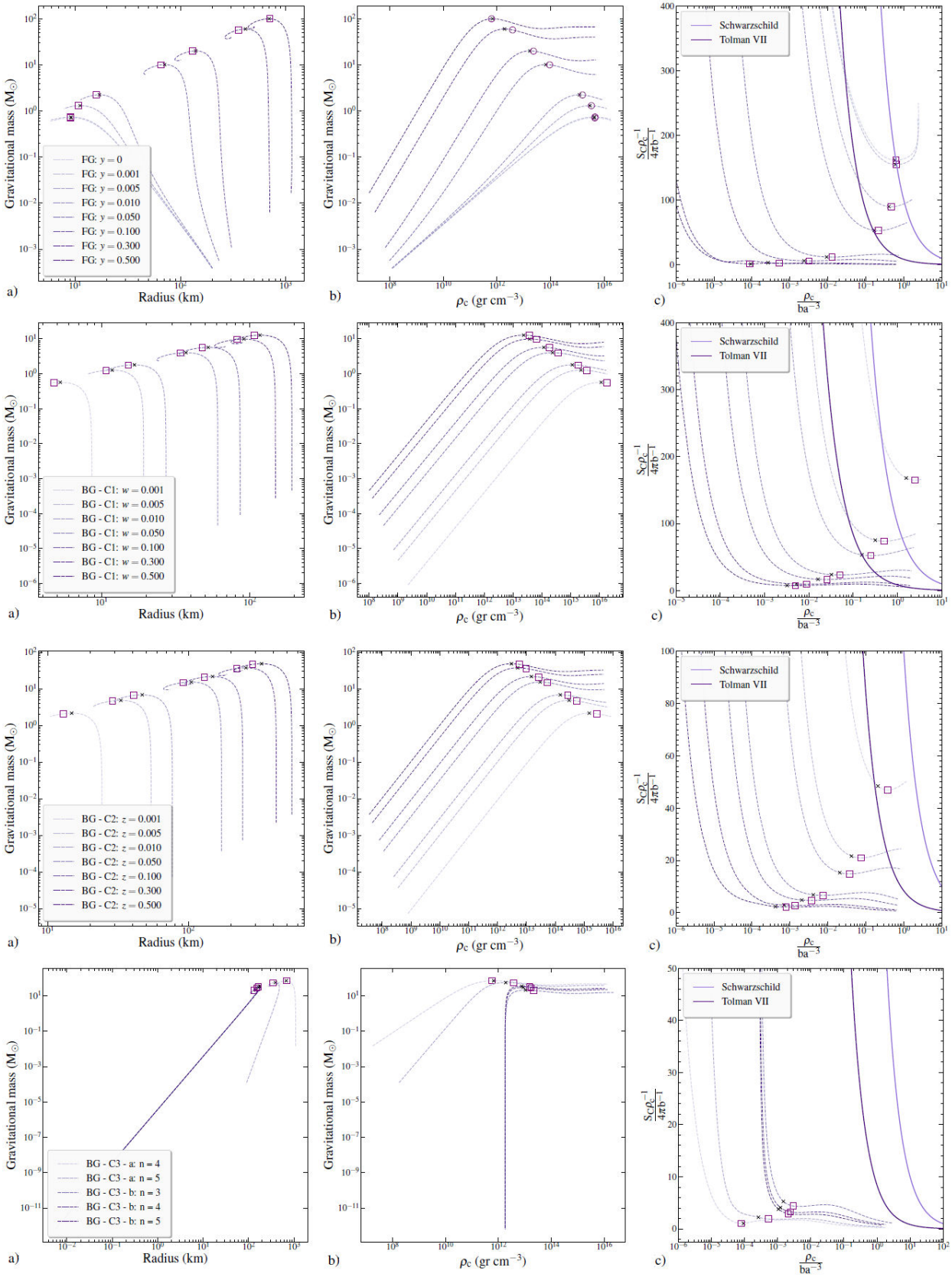

FIGURE 4. Same as the caption of Fig. 1, but for a set of FG EoSs (first panel), BG-C1 EoSs (second panel), BG-C2 EoSs (third panel), and BG-C3 EoSs (fourth panel).

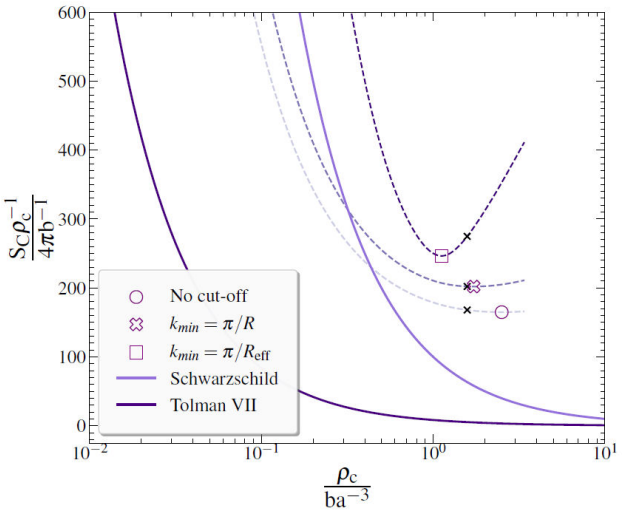

FIGURE 5. The CE as a function of the central density for the BG-C1 (0.001) EoS and two analytical solutions of TOV equations. The black crosses indicate the stability points due to the TM while the open markers correspond to the minimum of the CE with: a) no cutoff ($k_{\rm min} = 0$; circle), b) cutoff at $k_{\rm min} = \pi/R$ (cross), and c) cutoff at $k_{\rm min} = \pi/R_{\rm eff}$ (square).

the cutoff scheme in case (b) alters the behavior of the CE, leading to a sharper and more distinct outcome. Concluding, the choice of the momentum cutoff contributes significantly to the convergence of the two methods under consideration [45, 46].

6. Concluding remarks

The conclusions can be outlined as follows:

- CE serves as a partial indicator of the stability of compact objects such as neutron and quark stars, offering qualitative predictions of stability points. While its minimization provides an alternative approach to studying stability, the results remain non-quantitative due to their strong dependence on the EoS. A possible explanation, at least for neutron stars, is that the existence of the crust, which has a special constitutive explanation, has a dramatic effect on locating the stability point by the CE minimization method. On the other hand, in the case of quark stars, where there is no crust, the failure of the method does not currently have a solid explanation.

- In the case of fermionic or bosonic matter, the TM and CE methods for the location of the stability point converge with a good or moderate accuracy, for three out of four quantities under consideration. In fact, the most accurate prediction lies with the maximum mass, where the difference reaches values lower than 5%.

- As a key conclusion, the CE method serves as a qualitative rather than a quantitative tool for macroscopically identifying the instability region in certain compact object configurations. While it provides an alternative approach for exploring instability regions, its reliability is strongly influenced by the specific EoS and the internal structure of the compact star.

Acknowledgments

The authors would like to thank Dr. Nan Jiang for correspondence and useful comments. All numerical calculations were performed on a workstation equipped with 2 Intel Xeon Gold 6140 Processors (72 cpu cores in total) provided by the MSc program "Computational Physics" of the Physics Department, Aristotle University of Thessaloniki. This work was supported by the Croatian Science Foundation under Project No. HRZZ-MOBDOL-12-2023-6026, by the Croatian Science Foundation under Project No. IP-2022-10-7773, and by the Czech Science Foundation (GACR Contract No. 21-24281S).

1. J. Sañudo and A. Pacheco, Complexity and white-dwarf structure, *Phys. Lett. A* **373** (2009) 807, https://doi.org/10.1016/j.physleta.2009.01.008
2. K. Chatzisavvas *et al.*, Complexity and neutron star structure, *Phys. Lett. A* **373** (2009) 3901, https://doi.org/10.1016/j.physleta.2009.08.042
3. M. de Avellar and J. Horvath, Entropy, complexity and disequilibrium in compact stars, *Phys. Lett. A* **376** (2012) 1085, https://doi.org/10.1016/j.physleta.2012.02.012
4. M. de Avellar, *et al.*, Information theoretical methods as discerning quantifiers of the equations of state of neutron stars, *Phys. Lett. A* **378** (2014) 3481, https://doi.org/10.1016/j.physleta.2014.10.011
5. H. Adhitya and A. Sulaksono, Complexity and neutron stars with crust and hyperon core, *J. Phys.: Conf. Ser.* **1572** (2020) 012012, https://doi.org/10.1088/1742-6596/1572/1/012012
6. E. Contreras and E. Fuenmayor, Gravitational cracking and complexity in the framework of gravitational decoupling, *Phys. Rev. D* **103** (2021) 124065, https://doi.org/10.1103/PhysRevD.103.124065
7. C. Posada, J. Hladík, and Z. Stuchlík, Dynamical stability of the modified Tolman VII solution, *Phys. Rev. D* **103** (2021) 104067, https://doi.org/10.1103/PhysRevD.103.104067
8. L. Herrera, New definition of complexity for self-gravitating fluid distributions: The spherically symmetric, static case, *Phys. Rev. D* **97** (2018) 044010, https://doi.org/10.1103/PhysRevD.97.044010

9. L. Herrera, A. Di Prisco, and J. Ospino, Definition of complexity for dynamical spherically symmetric dissipative self-gravitating fluid distributions, *Phys. Rev. D* **98** (2018) 104059, https://doi.org/10.1103/PhysRevD.98.104059
10. L. Herrera, A. Di Prisco, and J. Ospino, Complexity factors for axially symmetric static sources, *Phys. Rev. D* **99** (2019) 044049, https://doi.org/10.1103/PhysRevD.99.044049
11. L. Herrera, A. Di Prisco, and J. Carot, Complexity of the Bondi Metric, *Phys. Rev. D* **99** (2019) 124028, https://doi.org/10.1103/PhysRevD.99.124028
12. M. Sharif and I. Butt, Complexity factor for charged spherical system, *Eur. Phys. J. C* **78** (2018) 688, https://doi.org/10.1140/epjc/s10052-018-6121-5
13. M. Sharif and I. I. Butt, Complexity factor for static cylindrical system, *Eur. Phys. J. C* **78** (2018) 850, https://doi.org/10.1140/epjc/s10052-018-6330-y
14. M. Sharif, A. Majid, and M. M. M. Nasir, Complexity factor for self-gravitating system in modified Gauss-Bonnet gravity, *Int. J. Mod. Phys. A* **34** (2019) 1950210, https://doi.org/10.1142/S0217751X19502105
15. M. Sharif and K. Hassan, Complexity of dynamical cylindrical system in f(G, T) gravity, *Mod. Phys. Lett. A* **37** (2022) 2250027, https://doi.org/10.1142/S0217732322500274
16. Z. Yousaf, M. Z. Bhatti, and T. Naseer, Study of static charged spherical structure in $f(R,T,Q)$ gravity, *Eur. Phys. J. Plus* **135** (2020) 323, https://doi.org/10.1140/epjp/s13360-020-00332-9
17. Z. Yousaf, *et al*., Influence of modification of gravity on the complexity factor of static spherical structures, *Mon. Not. R. Astron. Soc.* **495** (2020) 4334, https://doi.org/10.1093/mnras/staa1470
18. Z. Yousaf, M. Z. Bhatti, and T. Naseer, Measure of complexity for dynamical self-gravitating structures, *Int. J. Mod. Phys. D* **29** (2020) 2050061, https://doi.org/10.1142/S0218271820500613
19. Z. Yousaf, *et al*., Measure of complexity in self-gravitating systems using structure scalars, *New Astron.* **84** (2021) 101541, https://doi.org/https://doi.org/10.1016/j.newast.2020.101541
20. Z. Yousaf, M. Bhatti, and M. Nasir, On the study of complexity for charged self-gravitating systems, *Chin. J. Phys.* **77** (2022) 2078, https://doi.org/10.1016/j.cjph.2022.01.005
21. A. R. P. Moreira and S.-H. Dong, Probability measures of fermions on branes, *Eur. Phys. J. C* **83** (2023) 1064, https://doi.org/10.1140/epjc/s10052-023-12224-0
22. A. R. P. Moreira and S.-H. Dong, Brane stability under $f(Q,\mathcal{T})$ gravity, *Eur. Phys. J. C* **84** (2024) 1156, https://doi.org/10.1140/epjc/s10052-024-13552-5
23. A. R. P. Moreira, S.-H. Dong, and F. Ahmed, New mechanism for fermion localization in the presence of anti-curvature tensor, *Eur. Phys. J. C* **84** (2024) 913, https://doi.org/10.1140/epjc/s10052-024-13260-0
24. A. Moreira, F. Ahmed, and S.-H. Dong, Fermion localization on the brane in Ricci-inverse gravity, *Ann. Phys.* **469** (2024) 169763, https://doi.org/10.1016/j.aop.2024.169763
25. M. Gleiser and N. Stamatopoulos, Entropic measure for localized energy configurations: Kinks, bounces, and bubbles, *Phys. Lett. B* **713** (2012) 304, https://doi.org/10.1016/j.physletb.2012.05.064
26. M. Gleiser and D. Sowinski, Information-entropic stability bound for compact objects: Application to Q-balls and the Chandrasekhar limit of polytropes, *Phys. Lett. B* **727** (2013) 272, https://doi.org/10.1016/j.physletb.2013.10.005
27. M. Gleiser and N. Jiang, Stability bounds on compact astrophysical objects from information-entropic measure, *Phys. Rev. D* **92** (2015) 044046, https://doi.org/10.1103/PhysRevD.92.044046
28. M. Gleiser and D. Sowinski, Information-entropic signature of the critical point, *Phys. Lett. B* **747** (2015) 125, https://doi.org/10.1016/j.physletb.2015.05.058
29. N. R. Braga, Information versus stability in an anti-de Sitter black hole, *Phys. Lett. B* **797** (2019) 134919, https://doi.org/10.1016/j.physletb.2019.134919
30. N. R. F. Braga and R. da Mata, Configuration entropy for quarkonium in a finite density plasma, *Phys. Rev. D* **101** (2020) 105016, https://doi.org/10.1103/PhysRevD.101.105016
31. S. H. Alexander, K. Yagi, and N. Yunes, An entropy-area law for neutron stars near the black hole threshold, *Class. Quantum Grav.* **36** (2019) 015010, https://doi.org/10.1088/1361-6382/aaf14b
32. R. da Rocha, AdS graviton stars and differential configurational entropy, *Phys. Lett. B* **823** (2021) 136729, https://doi.org/10.1016/j.physletb.2021.136729
33. G. Karapetyan, The nuclear configurational entropy approach to dynamical QCD effects, *Phys. Lett. B* **786** (2018) 418, https://doi.org/10.1016/j.physletb.2018.09.058
34. R. A. C. Correa, *et al*., Configurational entropy as a constraint for Gauss-Bonnet braneworld models, *Phys. Rev. D* **94** (2016) 083509, https://doi.org/10.1103/PhysRevD.94.083509
35. W. Barreto, A. Herrera-Aguilar, and R. da Rocha, Configurational entropy of generalized sine-Gordon-type models, *Ann. Phys.* **447** (2022) 169142, https://doi.org/10.1016/j.aop.2022.169142
36. S. L. Shapiro and S. A. Teukolsky, Black Holes, White Dwarfs, and Neutron Stars (John Wiley & Sons, New York, 1983). https://doi.org/10.1002/9783527617661
37. N. Glendenning, Compact Stars: Nuclear Physics, Particle Physics, and General Relativity (Springer-Verlag, New York, 1997). https://doi.org/10.1007/978-1-4684-0491-3
38. P. Haensel, A. Potekhin, and D. Yakovlev, Neutron Stars 1: Equation of State and Structure (Springer-Verlag, New York, 2007). https://doi.org/10.1007/978-0-387-47301-7.

39. Y. Zeldovich and I. Novikov, Stars and Relativity (Dover Publications, INC, Mineapolis New York, 1971).
40. S. Weinberg, Gravitation and Cosmology: Principles and Applications of the General Theory of Relativity (John Wiley & Sons, New York, 1972).
41. B. Schutz, A First Course in General Relativity, 1st. ed., (Cambridge University Press, Cambridge, 1985).
42. J. Schaffner-Bielich, Compact Star Physics (Cambridge University Press, Cambridge, 2020). https://doi.org/10.1017/9781316848357
43. S. Chandrasekhar, The Dynamical Instability of Gaseous Masses Approaching the Schwarzschild Limit in General Relativity., *Astrophys. J.* **140** (1964) 417, https://doi.org/10.1086/147938
44. S. Chandrasekhar, Dynamical Instability of Gaseous Masses Approaching the Schwarzschild Limit in General Relativity, *Phys. Rev. Lett.* **12** (1964) 114, https://doi.org/10.1103/PhysRevLett.12.114
45. P. S. Koliogiannis, *et al*., Configurational entropy as a probe of the stability condition of compact objects, *Phys. Rev. D* **107** (2023) 044069, https://doi.org/10.1103/PhysRevD.107.044069
46. P. S. Koliogiannis, *et al*., Configurational entropy and stability conditions of fermion and boson stars, *Phys. Rev. D* **110** (2024) 104077, https://doi.org/10.1103/PhysRevD.110.104077
47. J. R. Oppenheimer and G. M. Volkoff, On Massive Neutron Cores, *Phys. Rev.* **55** (1939) 374, https://doi.org/10.1103/PhysRev.55.374
48. A. M. Raghoonundun and D. W. Hobill, Possible physical realizations of the Tolman VII solution, *Phys. Rev. D* **92** (2015) 124005, https://doi.org/10.1103/PhysRevD.92.124005
49. P. S. Negi and M. C. Durgapal, Stable Ultracompact Objects, *Gen. Relativ. Gravit.* **31** (1999) 13, https://doi.org/10.1023/A:1018807219245
50. P. Negi and M. Durgapal, Relativistic supermassive stars, *Astrophys. Space Sci.* **275** (2001) 185, https://doi.org/10.1023/A:1002707730439
51. C. Moustakidis, The stability of relativistic stars and the role of the adiabatic index, *Gen. Relativ. Gravit.* **49** (2017) 68, https://doi.org/10.1007/s10714-017-2232-9
52. P. S. Koliogiannis and C. C. Moustakidis, Effects of the equation of state on the bulk properties of maximally rotating neutron stars, *Phys. Rev. C* **101** (2020) 015805, https://doi.org/10.1103/PhysRevC.101.015805
53. C. Zhang and R. B. Mann, Unified interacting quark matter and its astrophysical implications, *Phys. Rev. D* **103** (2021) 063018, https://doi.org/10.1103/PhysRevD.103.063018
54. M. G. Alford, S. Han, and M. Prakash, Generic conditions for stable hybrid stars, *Phys. Rev. D* **88** (2013) 083013, https://doi.org/10.1103/PhysRevD.88.083013
55. S. Typel, Equations of state for astrophysical simulations from generalized relativistic density functionals, *J. Phys. G: Nucl. Part. Phys.* **45** (2018) 114001, https://doi.org/10.1088/1361-6471/aadea5
56. L. Tsaloukidis, *et al*., Twin stars as probes of the nuclear equation of state: Effects of rotation through the PSR J0952-0607 pulsar and constraints via the tidal deformability from the GW170817 event, *Phys. Rev. D* **107** (2023) 023012, https://doi.org/10.1103/PhysRevD.107.023012
57. G. Narain, J. Schaffner-Bielich, and I. N. Mishustin, Compact stars made of fermionic dark matter, *Phys. Rev. D* **74** (2006) 063003, https://doi.org/10.1103/PhysRevD.74.063003
58. M. Colpi, S. L. Shapiro, and I. Wasserman, Boson Stars: Gravitational Equilibria of Self-Interacting Scalar Fields, *Phys. Rev. Lett.* **57** (1986) 2485, https://doi.org/10.1103/PhysRevLett.57.2485
59. D. Rafiei Karkevandi *et al*., Bosonic dark matter in neutron stars and its effect on gravitational wave signal, *Phys. Rev. D* **105** (2022) 023001, https://doi.org/10.1103/PhysRevD.105.023001
60. S. Shakeri and D. R. Karkevandi, Bosonic dark matter in light of the NICER precise mass-radius measurements, *Phys. Rev. D* **109** (2024) 043029, https://doi.org/10.1103/PhysRevD.109.043029
61. P. Agnihotri, J. Schaffner-Bielich, and I. N. Mishustin, Boson stars with repulsive self-interactions, *Phys. Rev. D* **79** (2009) 084033, https://doi.org/10.1103/PhysRevD.79.084033
62. N. Rutherford *et al*., Constraining bosonic asymmetric dark matter with neutron star mass-radius measurements, *Phys. Rev. D* **107** (2023) 103051, https://doi.org/10.1103/PhysRevD.107.103051
63. S. L. Pitz and J. Schaffner-Bielich, Generating ultracompact boson stars with modified scalar potentials, *Phys. Rev. D* **108** (2023) 103043, https://doi.org/10.1103/PhysRevD.108.103043